Lecture 3.

Changes in planetary albedo. Is there a clear signal caused by aerosols and clouds?

<u>Outline</u>:

1. Background materials.

<u>2. Papers for class discussion</u>:

Palle et al., Changes in Earth's reflectance over the past two decades. Science, vol.304, pp.1299-1301, 28 May, 2004.

Wielicki et al., Changes in Earth's albedo measured by satellite. Science, vol. 308, p. 825, 6 May, 2005.

<u>Background materials.</u>

Planetary radiative equilibrium at the top of the atmosphere (TOA) (over the entire planet and long time interval, e.g., a year):

TOA outgoing radiation = TOA incoming radiation

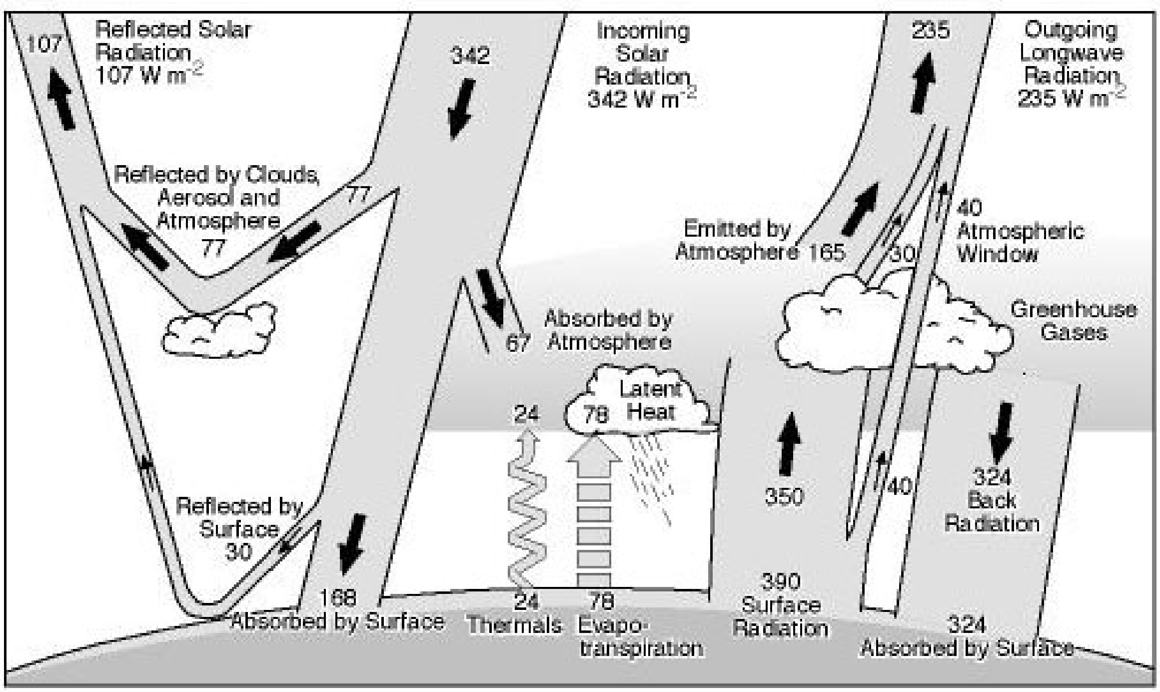

Figure 3.1 Earth's energy balance diagram from Kiehl J. and K. Trenberth, Earth's Annual Global Mean Energy Budget, *Bull. Amer. Meteor. Soc.*, **78**, 197-208, 1997.

TOA incoming radiation = TOA solar radiation – reflected solar radiation

If F_0 is the solar constant (i.e., solar flux at the top of the atmosphere), then incoming solar radiation (per unit area of Earth's surface) is

$$\mathbf{F_0\, \pi R_e^2 / 4\pi R_e^2 = F_0 / 4}$$

where Re is the radius of the Earth.

Assuming F_0 = 1368 W/m^2, TOA solar radiation is 1368 W/m^2/4 = <u>342 W/ m^2</u>

Then reflected solar radiation = $\alpha F_0 / 4$, where α is the global mean **planetary albedo**.

Taking α = 0.3, reflected solar radiation is 102.6 <u>W/ m^2</u>

<u>Incoming solar (shortwave) radiation at TOA:</u>

- ✓ Global average is 342 W/ m^2 (**F_0 /4)**
- ✓ Longitudinal (zonal) symmetry with uniform variation with latitude
- ✓ Hemispherical symmetry during equinox seasons with radiation increasing uniformly from equator to pole.
- ✓ Polar regions receive large amounts of radiation during summer (more that the equator, even during equinox) because of the length of the day

<u>Reflected solar radiation at TOA (see figure 3.2):</u>

- ✓ Longitudinal variations with non-uniform variations with latitude
- ✓ Weak hemispheric symmetry during equinox seasons
- ✓ Polar regions reflect largest amounts of radiation during summer, a result of high insolation but also high reflectivity
- ✓ Variations in longitude and non-uniform latitudinal behavior reflect changes in planetary albedo

<u>Planetary albedo (see figure 3.3)</u>

- ✓ The albedo field reflects the properties of the surface, and the distribution of aerosols and clouds.
- ✓ Albedo values are larger around the poles – a result of the reflective low clouds and snow/ice cover.
- ✓ Over the land, albedo is high over the arid (desert) areas and low in forest regions however, some of these forest regions are regions of deep and highly reflective clouds, which mask the surface properties to create high albedo.

- ✓ Over the tropical oceans, there are narrow regions of high albedo flaked by large regions of low albedo – evidence for narrowly confined cloud regions flaked by fast ocean areas with little cloudiness.

Figure 3.2 Reflected TOA solar radiation (satellite data).

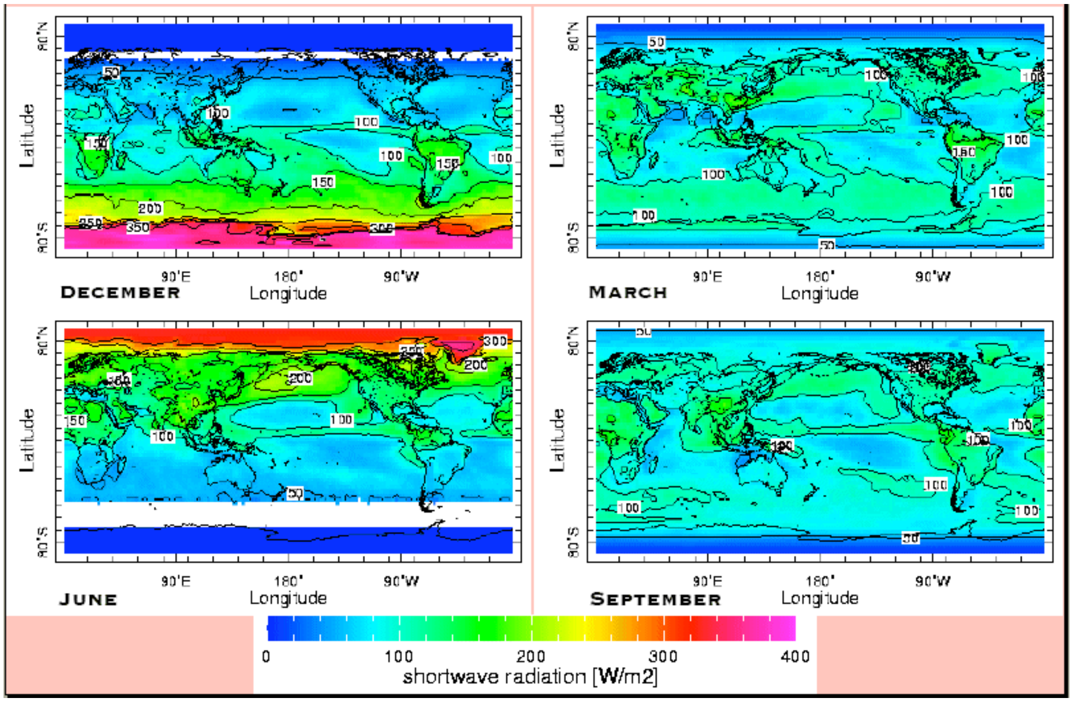

Figure 3.3 Planetary albedo

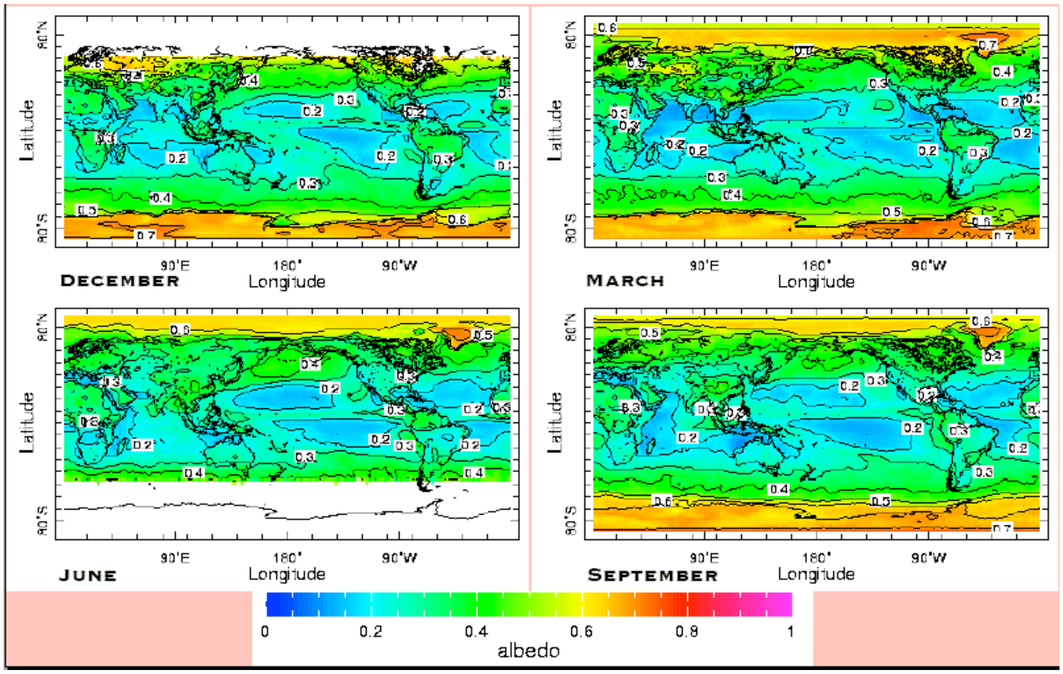

Radiative equilibrium at the top of the atmosphere (TOA) can be also defined as (net flux is zero)

$$F_{net}^{TOA} = \frac{F_0}{4}(1-\alpha) - F_{IR}^{\uparrow TOA} = 0$$

where $F_{IR}^{\uparrow TOA}$ is outgoing IR (thermal) flux (also called outgoing longwave radiation OLR). NOTE: Net flux is defined as the flux down minus flux up.

Radiative forcing, ΔF (W m^{-2}), is defined as a change of net radiative flux (longwave and shortwave) **at the top of the atmosphere** (see IPCC figure in Lecture 2. Time period: current – pre-industrial).

Net shortwave solar radiation (see figure 3.4)

- ✓ Global average 235 W/m^2 = $\frac{F_0}{4}(1-\alpha)$
- ✓ Results from the combination of the length-of-the-day, solar zenith angle, and local albedo.
- ✓ The poles are regions of minima (high albedo) and the tropics are regions of maxima, particularly over the vast subtropical areas, which are relatively cloud free and have low albedo.
- ✓ The distribution of the net shortwave is almost hemispherically symmetric with small variation in maximum with the season.

Outgoing longwave radiation (see figure 3.5):

- ✓ Global average 235 W/m^2 = $F_{IR}^{\uparrow TOA} = \frac{F_0}{4}(1-\alpha)$ - globally approximately

  balancing the net shortwave radiation over the course of the year (imbalances may occur during limited periods due to the ability of oceans to store heat away from the surface).
- ✓ OLR is more uniformly distributed with latitude than net shortwave, reflecting the planet's relatively uniform temperature – a direct result of the dynamical climate system, which works to distribute the heat received from the Sun around the globe.

- ✓ Regions with relatively little clouds and dry air upper atmosphere (subtropics) emit larger amounts of OLR to space
- ✓ Regions of deep clouds (Southeast Asia, South America, Africa) have the smallest OLR

Figure 3.4 Net shortwave (solar) radiation

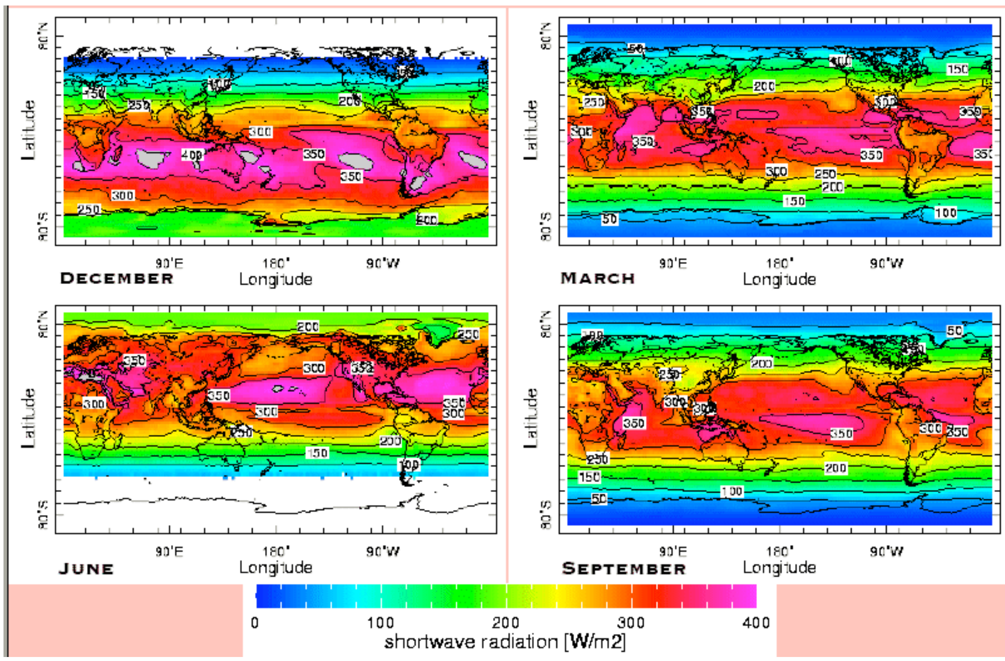

Figure 3.5 TOA outgoing longwave radiation.

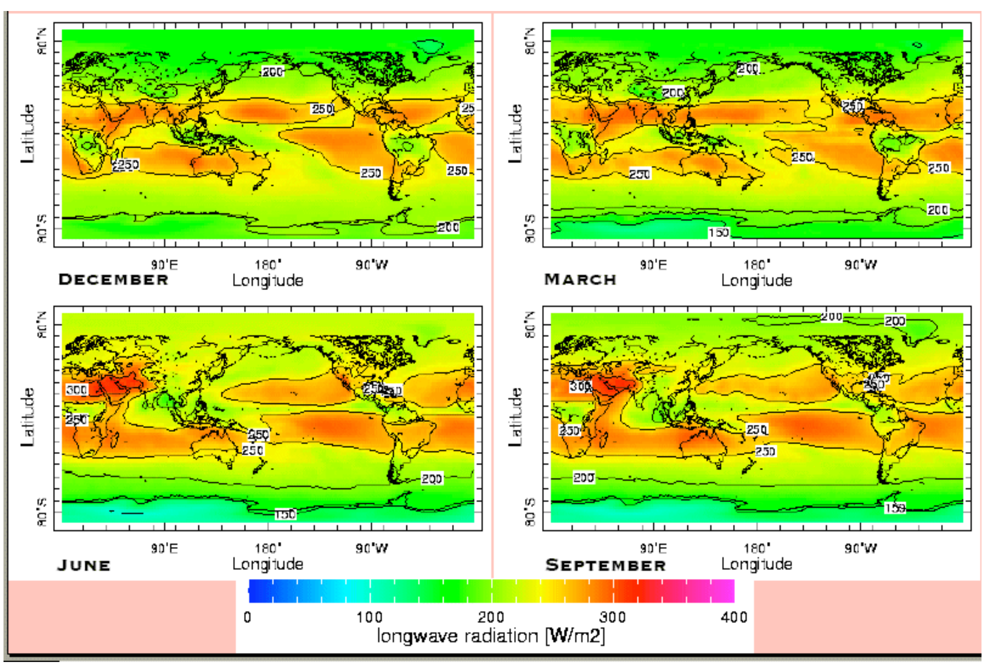

Satellite observations:

The **E**arth **R**adiation **B**udget **E**xperiment (**ERBE**) is made up of three satellites launched in the mid-1980s. Since then, ERBE has been the primary source of global data for studying the heating and cooling of the atmosphere.

The Clouds and the Earth's Radiant Energy System (**CERES**) was first launched in 1997 aboard TRMM, which flies in a near-equatorial orbit. Two more CERES sensors were launched in December 1999 aboard NASA's Terra satellite, which flies in a near-polar orbit. Terra's polar orbit allows CERES to measure the Earth's incoming and outgoing radiant energy on a global scale every day.

http://asd-www.larc.nasa.gov/ceres/ASDceres.html

http://earth-www.larc.nasa.gov/erbelike/

International Satellite Cloud Climatology Project (ISCCP): The purpose of ISCCP is to collect and analyze satellite observed radiances to infer the global distribution of radiative properties of clouds. The goal is to improve the modeling of cloud effects on climate. It uses data from the five geostationary satellites and polar orbiters of the NOAA/TIROS-N type (since July 1983).

http://isccp.giss.nasa.gov/